

Rheological response of a glass-forming liquid having large bidispersity

Vinay Vaibhav,^{1,2} Jürgen Horbach,³ and Pinaki Chaudhuri^{1,2}

¹*The Institute of Mathematical Sciences, CIT Campus, Taramani, Chennai 600113, India*

²*Homi Bhabha National Institute, Anushaktinagar, Mumbai 400094, India*

³*Institut für Theoretische Physik II, Heinrich-Heine-Universität Düsseldorf, Universitätsstraße 1, 40225 Düsseldorf, Germany*

Using extensive numerical simulations, we investigate the flow behaviour of a model glass-forming binary mixture whose constituent particles have a large size ratio. The rheological response to applied shear is studied in the regime where the larger species are spatially predominant. We demonstrate that the macroscopic rigidity that emerges with increasing density occurs in the regime where the larger species undergo a glass transition while the smaller species continue to be highly diffusive. We analyse the interplay between the timescale imposed by the shear and the quiescent relaxation dynamics of the two species to provide a microscopic insight into the observed rheological response. Finally, by tuning the composition of the mixture, we illustrate that the systematic insertion of the smaller particles affects the rheology by lowering of viscosity of the system.

I. INTRODUCTION

The rheological properties of soft glassy materials (colloids, gels, foams, emulsions, granular matter etc.) [1–7] are very important for a wide range of applications in our daily lives as well as in industries, and also lead to various natural phenomena. A characteristic feature of soft glassy materials is the existence of a yield stress, i.e. a threshold stress value which needs to be overcome to make the material flow. Once flowing, soft glasses typically behave as shear-thinning materials. Understanding the processes that lead to yielding and flow from a microscopic perspective is fundamental to our physical knowledge of the properties of soft glasses and could be utilized for the development of soft glasses that are functionalized towards specific applications.

Many soft glass systems consist of particles having a wide range of sizes. This is an important issue with respect to their mechanical properties. However, in experiments [8–11] and simulations [12–20] on the rheology of soft glasses, the focus has been on model systems with a moderate size dispersity. Here, the size dispersity has essentially been introduced to prevent the system from crystallization. However, recent studies [21, 22] have revealed that the degree of polydispersity has a strong impact on the glassy dynamics. In systems with a large polydispersity, there is a time-scale separation between the structural relaxation of large and small particles that leads to strong dynamical heterogeneities. How such a dispersity in particle size affects the rheological response is not well understood and needs to be further explored.

To address this issue, it is useful to consider disparate-sized binary mixtures. In the quiescent state, such systems are known to exhibit a complex phase behaviour [23] and a wealth of fascinating phenomena with respect to their glassy dynamics [24–28]. In the regime where the large particles predominantly occupy volume, there is a distinct difference in the dynamics of large and small particles as the density or packing fraction is increased.

The larger species are observed to undergo a glass transition first, while the smaller species remain highly diffusive. Subsequently, at much higher density, the smaller species reach dynamical arrest, with their motion reminiscent to the localization dynamics of tracer particles in an amorphous matrix of frozen-in soft spheres [29–31].

Only recently, there has been systematic experimental investigations of the transient and steady-state rheological response of binary colloidal mixtures having large size disparity between the constituent particles [32–36]. These investigations, typically done at a fixed volume fraction and using different shear protocols, reveal that the shear response changes varying the concentration of the smaller species. As long as the larger particles occupy more volume one observes a softening of the system, while it hardens when the volume occupied by the smaller species becomes predominant. This changing rheological response has been attributed to the change in local packing structures as the composition of the mixture is varied.

In this work, we report an extensive numerical study of the rheological behaviour of a model glass-forming binary mixture having large bidispersity, considering the regime where the larger particles predominantly occupy volume. We consider a model system where the two constituent species undergo separate dynamical arrests at vastly different densities [26]. We probe how the timescale introduced by the external shear interacts with the relaxation dynamics of the constituent species, which is then manifested in the flow behaviour. The main finding is that the measured rheological curves reveal the onset of macroscopic rigidity in the density regime where the larger particles undergo a mode coupling transition in the quiescent state. Importantly, when this rigidity is observed at macro-scale, the smaller species continue to express a fluid-like dynamics that is not affected by the external shear. Thus, there is a macroscopic solid-like response even though internally there still exists a fast dynamic species. Only at much larger densities, the external shear is seen to affect the dynamics of the smaller particles.

However, these fast particles do influence the rheology near the regime where rigidity sets in; we observe that the systematic insertion of the smaller particles into the mixture leads to a lowering of the viscosity, i.e. to the softening of the material, consistent with earlier experimental observations.

The paper is organised as follows. After the introductory discussion in Section I, the model system and the numerical methods are discussed in Section II. In Section III, we discuss our findings, with subsections on (i) recapitulation of equilibrium results that have been reported previously, (ii) elaboration of macroscopic and microscopic analysis of the response to applied shear, and (iii) illustration of how the smaller species influence the rheological response. Finally, in Section IV, we have a concluding discussion.

II. MODEL AND COMPUTER SIMULATION

The model glass-former that we consider for our study is a 50 : 50 binary mixture of repulsive particles whose quiescent dynamics has been well studied [26]. The bigger particles (labelled A) have a slight polydispersity in size to avoid crystallization; their diameters d_A are sampled from a uniform distribution, i.e., $d_A \in [0.85, 1.15]$. The diameter of the smaller particles (labelled B) are fixed to $d_B = 0.35$. The average size ratio of A and B particles is $\langle d_A \rangle / d_B \approx 2.85$ where $\langle d_A \rangle / \approx 1$. Details about the model interactions between these constituent particles, as well as the units for length, energy, and time can be found in Refs. [26, 37].

We study the rheological behaviour of this model system using molecular dynamics (MD) simulation via LAMMPS [38]. We consider a system consisting of $N = 2000$ particles in a three-dimensional box with periodic boundary conditions at constant temperature $T = 2/3$, which is maintained via a dissipative particle dynamics (DPD) thermostat [39]. The time step used for the simulations is $dt = 0.00075$. Initial states at different densities are sampled from our study on the quiescent behaviour of this system; see Ref. [37]. Apart from the 50:50 composition, we also study a couple of other compositions, viz. 100:0 and 75:25, in order to understand how the inclusion of B species changes the system's response to an external shear.

To investigate the rheological response of the system, we impose shear along the xy plane in the x -direction (see Fig. 1) using different shear rates ($\dot{\gamma}$) ranging between 1.5×10^{-6} and 10^{-3} . Lees-Edwards boundary conditions are utilised during the shearing. The rheological behaviour is studied for a range of densities varying from very small, viz. $\rho_A = 1.05$ to very large $\rho_A = 1.75$, where ρ_A is the partial density of A species. Note that all reported densities will be in terms of ρ_A , since we will be eventually probing how changing ρ_B influences the rhe-

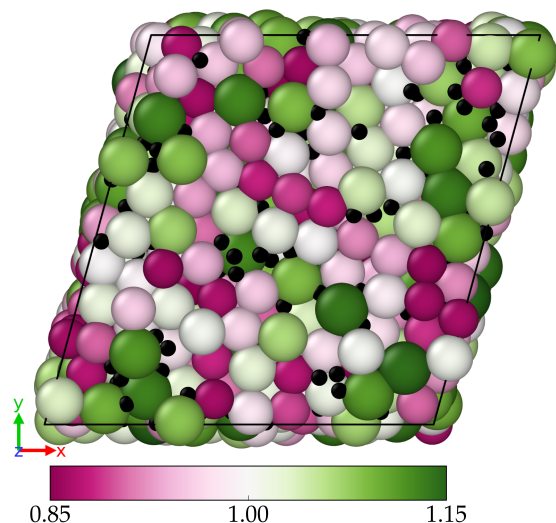


FIG. 1. *Snapshot of the sheared binary mixture.* The color panel represents the diameter of the polydisperse larger species (A). Smaller particles (B) are shown in black. The shear is applied in the x -direction along the xy plane.

ology at fixed ρ_A , as discussed above. A snapshot of the sheared system is shown in Fig. 1. As is evident, the larger species indeed populate most of the volume and the smaller species dot the intervening space. In this study, we inquire how the microscopic dynamics of these two species are manifested in the macro-rheology during the shear process.

III. RESULTS

Quiescent dynamics

As an introductory step, we summarize the dynamical behaviour observed by scanning across densities and monitoring the time evolution of the mean squared displacement (MSD) of the two species; see Fig. 2. As reported earlier in Ref. [26], the dynamics of the A species falls out of equilibrium around the critical density of mode coupling theory, $\rho_A^{\text{MCT}} = 1.115$). In the same density regime, the B species remain diffusive and undergo a dynamical arrest at a much higher density [26]. Or in other words, we observe two separate onsets of glassiness in the sub-populations, due to the large size ratio of the two species. Thus, at any density, the dynamics of the B species are faster than that of the A species, i.e., the relaxation timescales are relatively much slower. This large separation of timescales plays an important role in the rheological response, when a shear is introduced by driving the system at different shear-rates. The shear imposes a new timescale into the system and its interplay with the intrinsic timescale leads to the diversity in rheological response.

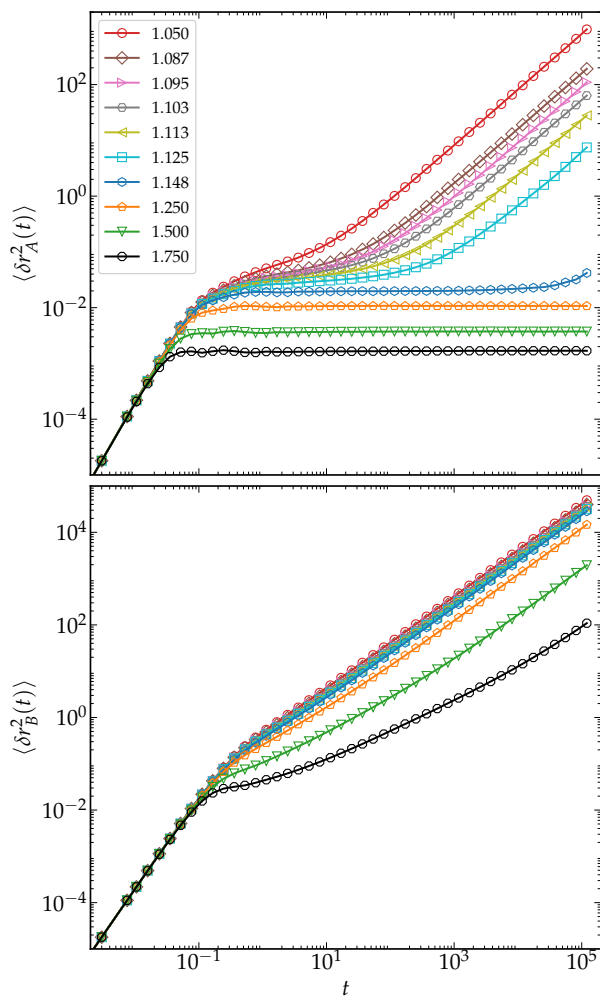


FIG. 2. *Quiescent dynamics.* Mean-squared displacement of bigger (upper panel) and smaller (lower panel) species of the unperturbed system i.e., in the absence of shear for different partial densities of bigger species. Densities are labelled in terms of partial density of A species ρ_A .

We also note here that for the A particles the MSD is measured in their center-of-mass reference frame. With this, we avoid finite-size effects in the high density regime, i.e. for $\rho > \rho_A^{\text{MCT}}$, occurring due to a relatively large center-of-mass diffusion coefficient of the A species for the considered relatively small system sizes. As a consequence, the A particles move collectively with their center of mass, despite their dynamical arrest with respect to particle rearrangements. For further discussion on this, see Ref. [37].

Steady-state macroscopic shear response

Next, we discuss the rheological response of the system over a range of densities and shear rates. A snapshot of the system during shear is shown in Fig. 1, with the large

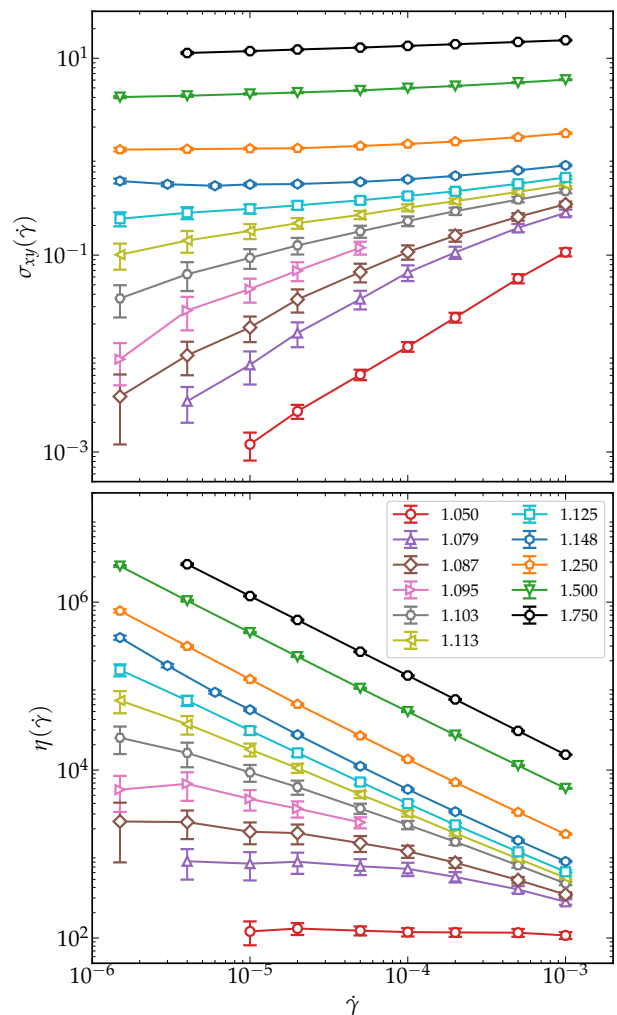


FIG. 3. *Rheological response.* Variation of steady-state shear stress σ_{xy} (top) and corresponding viscosity η (bottom) with applied shear-rate $\dot{\gamma}$, at different partial densities (ρ_A) of bigger species as marked.

size disparity of the two species distinctly visible.

Since the shear is imposed along the xy plane, we measure the corresponding shear stress σ_{xy} using the following Irving-Kirkwood expression: $\sigma_{xy} = \langle \frac{1}{V} \sum_{\alpha\beta} f_{\alpha\beta}^x r^y \rangle$, where $f_{\alpha\beta}^x$ is the x -component of the force with respect to a pair of particles and r^y is the y -component of the distance vector between two particles labelled α and β which could belong to either of the species A and B. V is the total volume of the simulated system. $\langle \cdot \rangle$ corresponds to averaging over states sampled in steady state.

At each density and imposed shear-rate, we obtain the steady state by shearing the system to large strains and then ensuring that the measured shear stress σ_{xy} fluctuates around a steady mean value. The data gathered for the variation of shear-stress with imposed shear rate, i.e., the flow curve, for the wide range of densities is shown in the top panel of Fig. 3. And, the corresponding viscosity defined by $\eta(\dot{\gamma}) = \sigma_{xy}(\dot{\gamma})/\dot{\gamma}$ is shown in the bottom panel

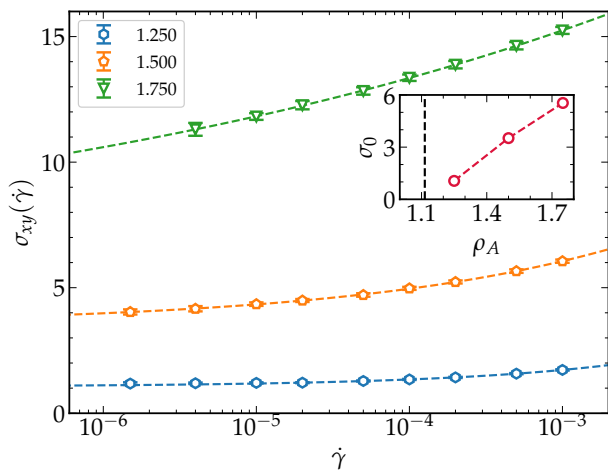


FIG. 4. *Herschel-Bulkley fits.* Flow curves, i.e., shear stress vs. strain-rate at different partial densities (ρ_A) of bigger species as marked, shown with corresponding Herschel-Bulkley fit ($\sigma = \sigma_0 + K\dot{\gamma}^n$) using dotted line. Fit estimates are $\sigma_0 = 1.06, 3.52, 5.54$, $K = 8.33, 13.92, 18.63$ and $n = 0.36, 0.25, 0.09$ for $\rho_A = 1.25, 1.50, 1.75$. (Inset) Variation of estimated value of yield stress σ_0 with ρ_A . Dotted vertical line marks ρ_A^{MCT} .

of Fig. 3.

The main findings from the rheological data are the following. At small densities ($\rho_A < 1.09$), a Newtonian regime, i.e., $\eta(\dot{\gamma})$ is constant, is observed at small shear-rates. At larger shear rates, shear thinning is observed, i.e., the viscosity decreases with increasing $\dot{\gamma}$. The Newtonian regime shrinks with increasing density, i.e., pushed to smaller and smaller shear rates. These are distinct characteristics of complex liquids. As the density is increased, an apparent yield stress becomes visible at $\rho_A \approx 1.125$, with σ_{xy} becoming flat with decreasing $\dot{\gamma}$. This implies that there is an onset of macroscopic rigidity for the binary mixture. Around this density regime, there is also a change in behaviour of $\eta(\dot{\gamma})$ – within the window of small shear rates, the viscosity continues to be an increasing function, i.e., there is no tendency to change curvature towards plateauing out. With further increase of density, the apparent yield stress of the system, viz. $\sigma_{xy}(\dot{\gamma} \rightarrow 0)$, increases steadily, which is characteristic to amorphous solids. One can fit the variation of stress with shear rate in this large density regime using the Herschel-Bulkley (HB) function, $\sigma = \sigma_0 + K\dot{\gamma}^n$, where σ_0 is the estimated yield stress, K is a constant and n is the HB exponent. The fits to the measured data for different ρ_A are shown in Fig. 4 and the values of the fit parameters are listed in the caption. In the inset of Fig. 4, we display the emergence and increase of the estimated yield stress σ_0 with density, beyond ρ_A^{MCT} .

Overall, such variation of rheological flow curves, viz. the emergence of a yield stress with the variation in a control parameter (e.g. temperature or packing fraction

or density) are very similar to the ones obtained in other soft-sphere glassy systems [13, 19, 20, 40].

Steady-state microscopic dynamics

In order to further analyse the rheological response, we study the microscopic dynamics of the system in steady state. In the vorticity direction, i.e., normal to the shear plane, we compute the MSD for the A and B species, separately, as well as the self part of the van Hove function of which MSD is the second moment. The van Hove Function, $G_s(r, t)$ is measured at a late time ($t = 8075.4$) in each case. The corresponding aggregated plots showing the variation of the dynamics with changing density are shown in Fig. 5, for MSD and $G_s(r, t)$, for a range of imposed shear rates. All measurements are done in the center-of-mass reference of respective species, to remove the effects resulting from finite center-of-mass diffusion in the glassy regime of A species.

At the smaller density ($\rho_A = 1.0500$), we do not observe any variation in the dynamics with imposed shear rate, for both A and B species, and the MSD curves as well as the $G_s(r, t)$ data are indistinguishable between the equilibrium and non-equilibrium regimes. This corresponds to the linear response regime, which is characterised by the Newtonian viscosity, see Fig. 5 (a), (d) for the MSD data and the corresponding data for $G_s(r, t)$ in Fig. 5 (g), (j).

If we now consider the higher density, $\rho_A = 1.1125$, which is in the vicinity of ρ_A^{MCT} , we observe that for the B species, the indistinguishability between the equilibrium and non-equilibrium data for MSD and $G_s(r, t)$ continue, i.e., the external shear is having no effect; see Fig. 5 (e), (k). However, for the A species, the shear introduces deviation from equilibrium behaviour, with an enhancement in long-time diffusive dynamics with increasing shear rate, as is visible in the MSD data (Fig. 5 (b)) which is also evident in the distinct change in the shape of the corresponding $G_s(r, t)$ (Fig. 5(h)). Thus, at this density, the imposed shear rate corresponds to a timescale which is faster than the equilibrium relaxation timescale of the A species, which is not the case for B species. Note that, for this density, an apparent macroscopic yield stress is visible. Thus, we can conclude that the apparent emergence of macroscopic rigidity and subsequent yielding under shear is a consequence of the interplay between the external drive and the structure formed by the A species, while the B species remain oblivious to this process and thus seems inconsequential to the overall rheological response, i.e., variation of viscosity with shear rate in this density regime.

However, if we go to even larger densities, $\rho_A = 1.7500$, the imposed shear affects the dynamics of both the A and B species; see Fig. 5 (c), (f), (i), (l); for both species, enhanced diffusion is observed with increasing shear rate.

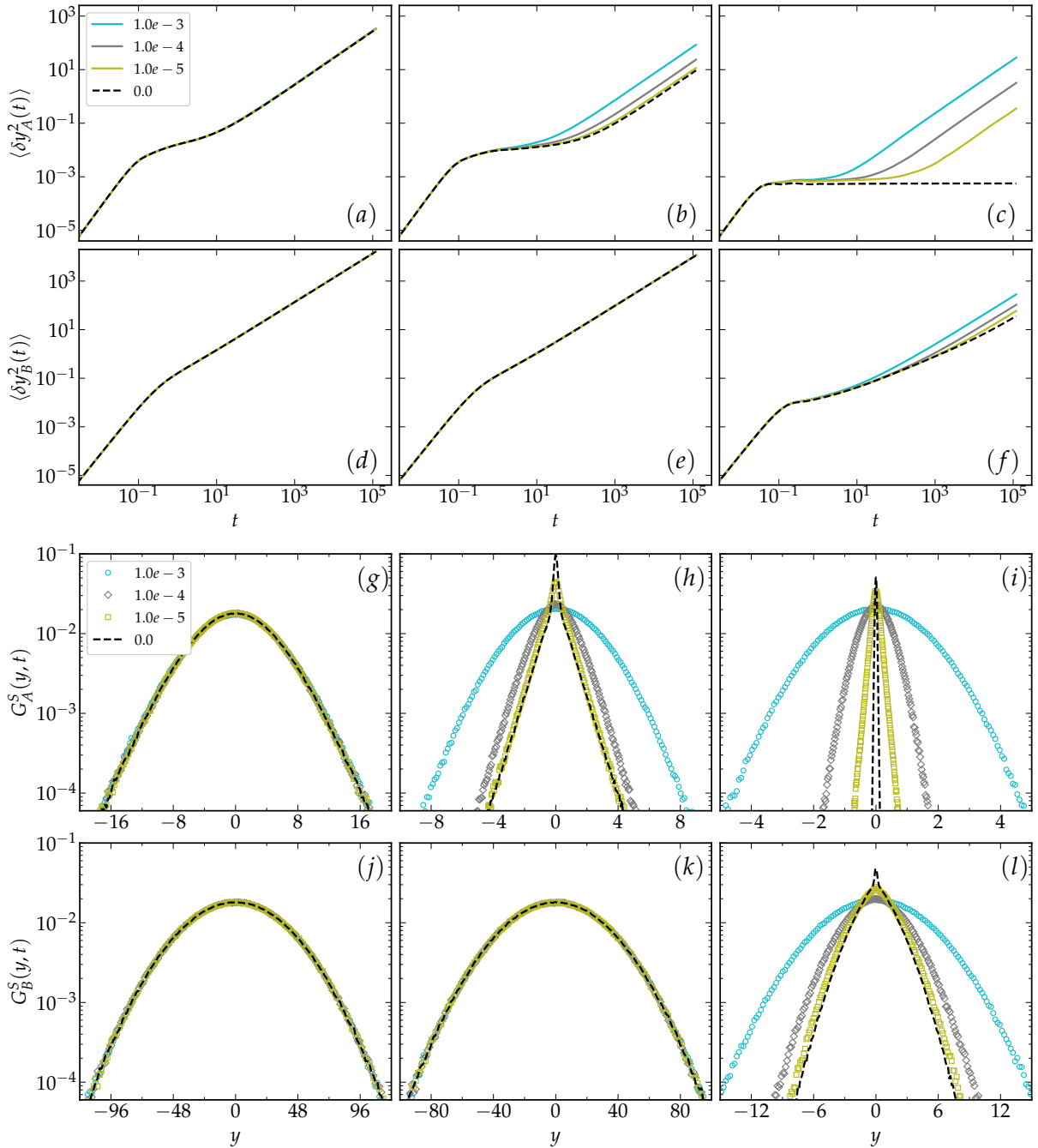


FIG. 5. *Microscopic dynamics under applied shear*: Mean squared displacement of bigger (a-c) and smaller (d-f) species in the presence (with solid lines) and in the absence (with dotted lines) of shear, measured in the vorticity direction. Corresponding self part of van Hove function, $G_s(y, t)$ of bigger species (g-i) and smaller (j-l) species in the presence (with symbols) and absence (dotted lines) of shear, at $t = 8075.4$, also measured in the vorticity direction. In both cases, first column represents system at partial density $\rho_A = 1.0500$, middle at $\rho_A = 1.1125$ and last at $\rho_A = 1.7500$.

Thus, the imposed timescales via the shear are faster compared to the equilibrium relaxation timescale for both species, even though there is still a large separation in dynamical timescales in the quiescent state.

We can extract a diffusion coefficient from the long-time diffusive dynamics observed in the MSD data, for

the various imposed shear rates at different densities. The shear-rate dependence of the diffusion constant, for the range of densities explored, is shown in Fig. 6, for both A and B species.

At small densities, the diffusion coefficient for both A and B species has no shear-rate dependence, which is just

a reflection of the fact that the dynamics remains unaffected by the shear, as discussed above. This behaviour continues for B species up to very large densities where the shear starts to have an effect. Also, in this density regime, the diffusion coefficient for A species has a power-law dependence on shear rate and appears to vanish at $\dot{\gamma} \rightarrow 0$, which is typical to the shear response of amorphous systems. In the intermediate density regime, the diffusion coefficient also decreases with decreasing shear rate, but deviates from a power-law behaviour and seems to reach a constant at vanishing shear rates. This would imply that there is a diffusive behaviour in the absence of shear at these densities. This behaviour is observed around the density where the onset of glassiness occurs for the A species, viz. in the vicinity of ρ_A^{MCT} . We also note that for B species a similar behaviour is observed at the largest density that we have explored, implying that in the absence of shear, the smaller particles would be undergoing equilibrium diffusive dynamics in that density regime.

To summarise, from the rheological response of the binary mixture, we infer that beyond ρ_{MCT} , an apparent yield stress emerges which is linked to the glassiness undergone by the A species. On contrary, the B species continue to be very mobile inside the matrix formed by the A species and their dynamics does not couple to the shear, and thus their contribution to the system's shear response is minimal. Only at much higher densities, the yielding process involves the collective interplay of both A and B species.

Role of smaller species: varying the composition

We now address the question of what role do the B species play in the rheological response. We address this questions by varying the composition of the mixture, and even considering the situation where the B species are completely absent.

We begin by first examining how the equilibrium behaviour of the system is influenced by the presence or absence of the B species. In the top panel of Fig. 7, we show the MSD data for the A species for varying A:B compositions, viz. 100:0, 75:25 and 50:50 for three different ρ_A . We note that at small densities, there is no variation in the dynamics, but at relatively larger densities ($\rho_A = 1.113$) there is distinct variation with the long-time dynamics becoming faster with increased presence of B species. This is also reflected in the measured diffusion coefficients as shown in the inset of the top panel of Fig. 7. From this data, it would imply that ρ_A^{MCT} shifts to larger densities with the increasing inclusion of B species. It is interesting to note that, the insertion of the smaller B species has a very different effect than insertion of bigger particles in a system of smaller particles. In the latter case, the bigger particles act as pinning sites

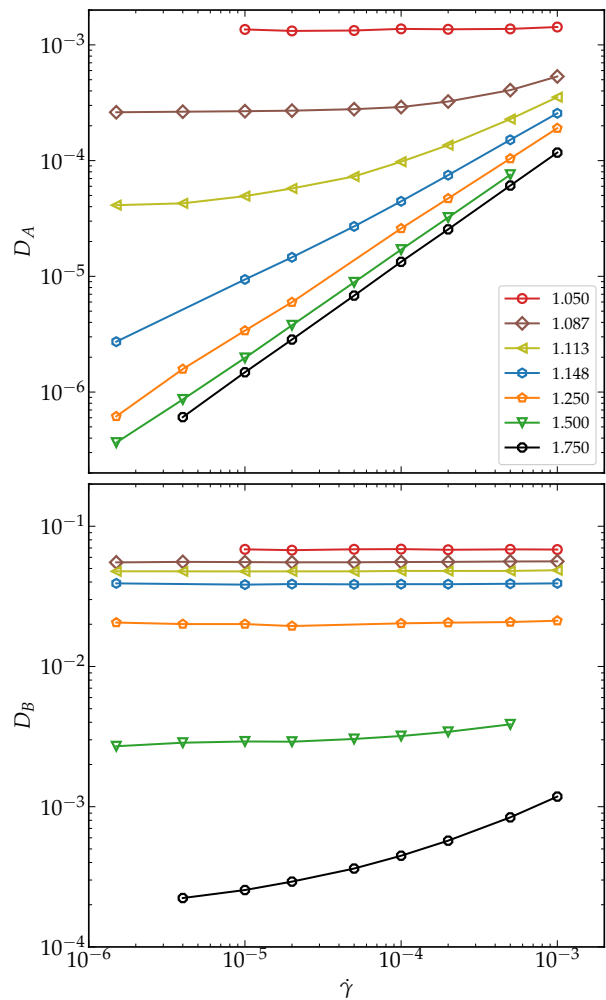


FIG. 6. *Diffusion coefficient in the presence of shear.* Variation of diffusion coefficient of bigger (top) and smaller (bottom) species with shear rate, measured in the vorticity direction, at different partial densities of bigger species as marked.

and slow down the dynamics.

Next, we study how the rheological response changes, in the presence or absence of the small particles. In the bottom panel of Fig. 7, we do a comparison of the rheological curves for the different compositions listed above. The effect of enhancement in equilibrium dynamics due to the presence of B species is reflected in the rheology data, especially in the intermediate density regime (as the glassy regime of A species is approached), where the viscosity of the system distinctly decreases at small shear rates with increasing presence of B species. This effect is absent at small densities and also at very large densities where the entire system becomes glassy. Thus, in the intermediate density regime, the mobile B population does have a softening effect on the overall shear response, an effect which can be exploited in various applications.

Our findings are consistent with experiments involving

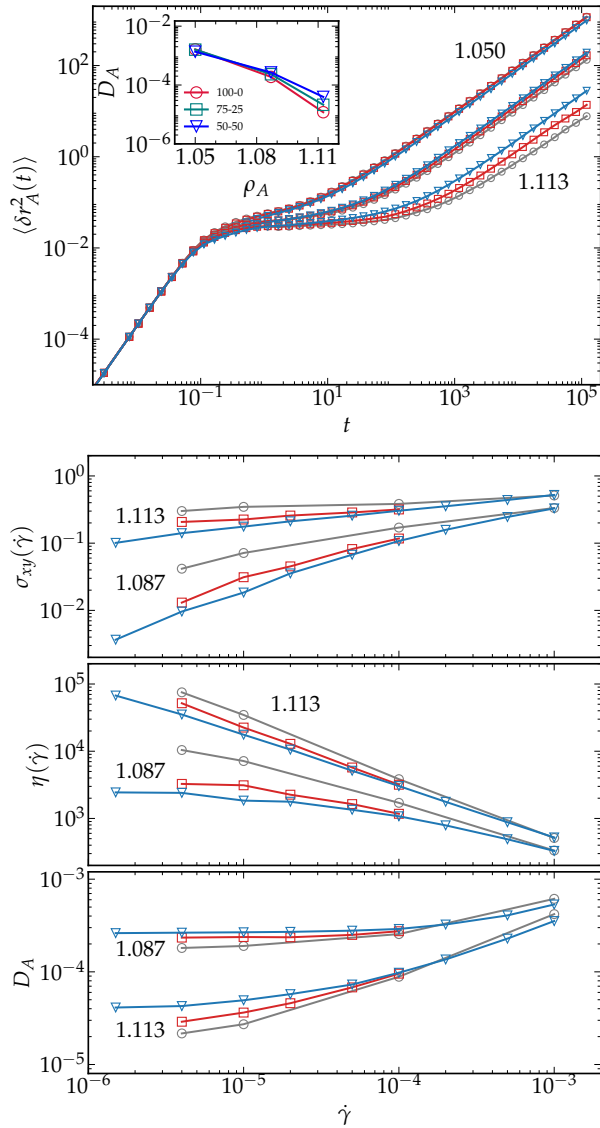


FIG. 7. *Effect of varying composition.* (Top) *Quiescent behavior.* MSD measured for the A species, for different composition of the mixture (circle: 100-0, square: 75-25, triangle: 50-50). (Inset) Variation of larger particle diffusion coefficient with partial density ρ_A for different composition of the system. (Bottom) *Rheological response.* Shear stress and viscosity as a function of shear-rate for different composition of the mixture. And, diffusion coefficient versus shear rate for the same compositions.

colloidal glasses with constituents having large size ratio, where a similar softening of the material was observed with increasing insertion of small particles till a 50:50 composition was reached [35, 36].

IV. CONCLUSIONS AND PERSPECTIVE

In conclusion, we have studied the shear response of a glass forming model binary mixture having a large size

ratio between the constituent species. The mixture having a composition of 50:50 corresponds to the case where the larger species occupy most of the volume. For such a system, it had earlier been demonstrated that as the overall density is increased, the larger particles undergo dynamical arrest first while the small particles continue to be diffusive within the matrix formed by the large ones. In our study, we probe how the external drive applied via a fixed shear rate, of varying magnitude, influences this microscopic dynamics and how that manifests in the observed steady-state rheological response.

The main observation comes via the measured shear stress, in steady state, as a function of the imposed shear rate. At small densities, the low shear-rate regime corresponds to that of a Newtonian fluid. However, in the density regime where the larger species within the mixture undergo a mode coupling dynamical transition in the quiescent state, the shape of the flow curves change at vanishing shear rates and an effective yield stress can clearly be estimated. Thus, there is a macroscopic rigidity. If we now focus on the microscopic dynamics, we observe that while the motion of the larger species indeed get influenced by the external shear, the dynamics of the smaller species remain completely unchanged vis-a-vis their motion in the absence of shear, within the explored range of shear rates. Thus, the macroscopic rigidity at vanishing shear rate is occurring while there is a highly mobile population of the smaller species within the system.

With increasing density, the yield stress increases as expected and the diffusion coefficient of the larger species exhibit a distinct power-law behaviour as a function of applied shear rate which is a distinctive feature of glassy systems. Only at large densities, we start to observe that the external shear rate is able to influence the motion of the smaller species, i.e., the timescale imposed by the applied shear rate is large enough to compete with the relaxation timescale of the smaller species.

Finally, we probe the role of the smaller species in the rheological response of the mixture, since the macroscopic rigidity emerges in the system even though these particles remain highly mobile. We observe that if we start with a system of just the large particles and then start inserting the smaller species, i.e., systematically change the mixture's composition, the rheological response changes in the small shear-rate regime, viz. the viscosity of the system decreases. Thus, the presence of the smaller particles softens the mixture's mechanical response, which is consistent with experimental observation in similar colloidal mixtures. Note that similar plasticizing effects have also been reported for polymeric systems [41, 42] where the inclusion of very small colloidal particles led to softening. Hence, this indicates to a very generic mechanism at play in how such inclusions can influence rheology. We also note here that this behaviour is in contrast to the situation where the inclusion of large

particles in a matrix of small particles can lead to hardening of the system, i.e., the rheological behaviour of the mixture changes as the composition is changed.

The next step should be to study the flow behaviour of glass forming liquids where particles have large polydispersity in size [22, 43], to investigate how our findings on the connection between microscopic dynamics and macroscopic mechanical response get translated to more complex mixtures. Also, there is a need to study how thermal fluctuations influence rheology in such mixtures, by comparing the response in the athermal limit where there have been some initial studies on probing the jamming behaviour, the plasticity and also the shear response in asymmetric binary mixtures [44–48].

ACKNOWLEDGMENTS

We acknowledge the use of HPC facility at IMSc Chennai for our computational work.

-
- [1] R. G. Larson, *The structure and rheology of complex fluids* (Oxford Univ. Press, New York, 1999).
- [2] D. T. Chen, Q. Wen, P. A. Janmey, J. C. Crocker, and A. G. Yodh, *Annu. Rev. Condens. Matter Phys.* **1**, 301 (2010).
- [3] D. Bonn, M. M. Denn, L. Berthier, T. Divoux, and S. Manneville, *Rev. Mod. Phys.* **89**, 035005 (2017).
- [4] Y. Joshi and G. Petekidis, *Rheol. Acta* **57**, 521 (2018).
- [5] P. Coussot, *J. Non-Newton. Fluid Mech.* **211**, 31 (2014).
- [6] A. Nicolas, E. E. Ferrero, K. Martens, and J.-L. Barrat, *Rev. Mod. Phys.* **90**, 045006 (2018).
- [7] D. Rodney, A. Tanguy, and D. Vandembroucq, *Model. Simul. Mater. Sci. Eng.* **19**, 083001 (2011).
- [8] G. Petekidis, A. Moussaid, and P. N. Pusey, *Phys. Rev. E* **66**, 051402 (2002).
- [9] R. Besseling, E. R. Weeks, A. B. Schofield, and W. C. K. Poon, *Phys. Rev. Lett.* **99**, 028301 (2007).
- [10] P. Schall, D. A. Weitz, and F. Spaepen, *Science* **318**, 1895 (2007).
- [11] V. Chikkadi and P. Schall, *Phys. Rev. E* **85**, 031402 (2012).
- [12] R. Yamamoto and A. Onuki, *Phys. Rev. E* **58**, 3515 (1998).
- [13] L. Berthier and J. L. Barrat, *J. Chem. Phys.* **116**, 6228 (2002).
- [14] F. Varnik, L. Bocquet, and J. L. Barrat, *J. Chem. Phys.* **120**, 2788 (2004).
- [15] G. P. Shrivastav, P. Chaudhuri, and J. Horbach, *Phys. Rev. E* **94**, 042605 (2016).
- [16] G. P. Shrivastav, P. Chaudhuri, and J. Horbach, *J. Rheol.* **60**, 835 (2016).
- [17] P. Leishangthem, A. D.S. Parmar, and S. Sastry, *Nat. Commun.* **8**, 14653 (2017).
- [18] M. L. Falk and J. S. Langer, *Phys. Rev. E* **57**, 7192 (1998).
- [19] A. Ikeda, L. Berthier, and P. Sollich, *Phys. Rev. Lett.* **109**, 018301 (2012).
- [20] A. Ikeda, L. Berthier, and P. Sollich, *Soft Matter* **9**, 7669 (2013).
- [21] E. Zaccarelli, S. M. Liddle, and W. C. K. Poon, *Soft Matter* **11**, 324 (2015).
- [22] D. Heckendorf, K. J. Mutch, S. U. Egelhaaf, and M. Laurati, *Phys. Rev. Lett.* **119**, 048003 (2017).
- [23] A. Imhof and J. K. G. Dhont, *Phys. Rev. Lett.* **75**, 1662 (1995).
- [24] A. J. Moreno and J. Colmenero, *J. Chem. Phys.* **125**, 164507 (2006).
- [25] A. J. Moreno and J. Colmenero, *Phys. Rev. E* **74**, 021409 (2006).
- [26] J. Horbach and T. Voigtmann, *Phys. Rev. Lett.* **109**, 205901 (2009).
- [27] J. Hendricks, R. Capellmann, A. B. Schofield, S. U. Egelhaaf, and M. Laurati, *Phys. Rev. E* **91**, 032308 (2015).
- [28] E. Lázaro-Lázaro, J. A. Perera-Burgos, P. Laermann, T. Sentjabrskaja, G. Pérez-Ángel, M. Laurati, S. U. Egelhaaf, M. Medina-Noyola, T. Voigtmann, R. Castañeda-Priego, and L. F. Elizondo-Aguilera, *Phys. Rev. E* **99**, 042603 (2019).
- [29] T. O. E. Skinner, S. K. Schnyder, D. G. A. L. Aarts, J. Horbach, and R. P. A. Dullens, *Phys. Rev. Lett.* **111**, 128301 (2013).
- [30] S. K. Schnyder, T. O. E. Skinner, A. L. Thorneywork, D. G. A. L. Aarts, J. Horbach, and R. P. A. Dullens, *Phys. Rev. E* **95**, 032602 (2017).
- [31] S. K. Schnyder and J. Horbach, *Phys. Rev. Lett.* **120**, 078001 (2018).
- [32] T. Sentjabrskaja, D. Guu, M. P. Lettinga, S. U. Egelhaaf, and M. Laurati, *AIP Conf. Proc.* **1518**, 206 (2013).
- [33] T. Sentjabrskaja, E. Babaliari, J. Hendricks, M. Laurati, G. Petekidis, and S. U. Egelhaaf, *Soft Matter* **9**, 4524 (2013).
- [34] T. Sentjabrskaja, M. Hermes, W. C. K. Poon, C. D. Estrada, R. Castañeda-Priego, S. U. Egelhaaf, and M. Laurati, *Soft Matter* **10**, 6546 (2014).
- [35] T. Sentjabrskaja, J. Hendricks, A. R. Jacob, G. Petekidis, S. U. Egelhaaf, and M. Laurati, *J. Rheol.* **62**, 149 (2018).
- [36] T. Sentjabrskaja, A. R. Jacob, S. U. Egelhaaf, G. Petekidis, T. Voigtmann, and M. Laurati, *Soft Matter* **15**, 2232 (2019).
- [37] V. Vaibhav, J. Horbach, and P. Chaudhuri, *arXiv:2202.12189*.
- [38] S. Plimpton, *J. Comp. Phys.* **117**, 1 (1995).
- [39] T. Soddemann, B. Dünweg, and K. Kremer, *Phys. Rev. E* **68**, 046702 (2003).
- [40] M. Golkia, G. Shrivastav, P. Chaudhuri, and J. Horbach, *Phys. Rev. E* **102**, 023002 (2020).
- [41] E. Zaccarelli, C. Mayer, A. Asteriadi, C. N. Likos, F. Sciortino, J. Roovers, H. Iatrou, N. Hadjichristidis, P. Tartaglia, H. Löwen, and D. Vlassopoulos, *Phys. Rev. Lett.* **95**, 268301 (2005).
- [42] J. T. Kalathi, G. S. Grest, and S. K. Kumar, *Phys. Rev. Lett.* **109**, 198301 (2012).
- [43] S. K. Behera, D. Saha, P. Gadige, and R. Bandyopadhyay, *Phys. Rev. Mater.* **1**, 055603 (2017).
- [44] S. Pednekar, J. Chun, and J. F. Morris, *J. Rheol.* **62**, 513 (2018).
- [45] Y. Hara, H. Mizuno, and A. Ikeda, *Phys. Rev. Res.* **3**, 023091 (2021).
- [46] J. C. Petit, N. Kumar, S. Luding, and M. Sperl, *Phys. Rev. Lett.* **125**, 215501 (2020).

[47] N. Xu and E. S. C. Ching, *Soft Matter* **6**, 2944 (2010).

[48] J. Clara-Rahola, T. A. Brzinski, D. Semwogerere, K. Feitosa, J. C. Crocker, J. Sato, V. Breedveld, and E. R. Weeks, *Phys. Rev. E* **91**, 010301(R) (2015).